Carbohydrate Polymers 98 (2013) 43–49

Contents lists available at SciVerse ScienceDirect

Carbohydrate Polymers

journal homepage: www.elsevier.com/locate/carbpol

Hydrolysis of wheat B-starch and characterisation of acetylated maltodextrin

Petra Smrčková[a], Jiří Horský[b], Evžen Šárka[a,*], Jaroslav Koláček[a], Miloš Netopilík[b], Zuzana Walterová[b], Zdeněk Kruliš[b], Andrey Synytsya[a], Kateřina Hrušková[b]

[a] Institute of Chemical Technology, Department of Carbohydrates and Cereals, Technická 5, 166 28 Prague 6, Czech Republic
[b] Institute of Macromolecular Chemistry, Academy of Sciences of the Czech Republic, Heyrovsky Sq. 2, 162 06 Prague 6, Czech Republic

ARTICLE INFO

Article history:
Received 4 February 2013
Received in revised form 8 April 2013
Accepted 17 April 2013
Available online 13 May 2013

Keywords:
Wheat B-starch
α-Amylase
Acetylated maltodextrin
Uniformity

ABSTRACT

Wheat B-starch was hydrolysed by α-amylase "Liquozyme supra" from *Bacillus licheniformis* at 90 °C and pH 7. After 2 h, the dextrose equivalent was 18; according to size exclusion chromatography, however, the hydrolysate contained not only dominant malto-oligosaccharides with the degree of polymerisation (*DP*) < 10 but also more than 20% of components with *DP* higher than 40. The product was acetylated to a high degree as verified by FTIR and ^{1}H NMR (degree of substitution *DS* = 3.1); nevertheless, detailed analysis of the MALDI-TOF mass spectra of the product showed that most of the malto-oligosaccharides molecules contained one or two residual hydroxyls. Size exclusion chromatography confirmed that the acetylated maltodextrin still contained a significant part with *DP* > 40. This non-uniformity of acetylated maltodextrin, both with respect to *DP* and to *DS*, must be taken into account in the development of acetylated-maltodextrin applications such as use as plasticisers or compatibilisers in biodegradable composites.

1. Introduction

Wheat starch comprises two types of granules: (i) larger lenticular granules with a diameter of 20–30 μm (A-starch) and (ii) smaller spherical granules of 2–8 μm in diameter (B-starch) (Leeb & Schumann, 2007). Industrially produced B-starch is a by-product of specific quality. Due to unavoidable impurities it owns a higher concentration of protein, lipids and pentosans and has a higher affinity to water at room temperature (Galliard, Bowler, & Towersey, 1994; Knight & Olson, 1984).

Processing of B-starch is problematic with respect to certain unit operations of typical starch refining (filtration, drying, etc.). Industrial and food applications are therefore limited. Thus, B-starch is used as cattle feed – e.g. milk substitute in calf feeds – as a core binder in foundries, as a binding agent in the production of corrugated boards, or as a raw material for the production of ethanol (Šárka & Bubník, 2010). As the amount of B-starch produced in wheat starch factories is about 10% of the total amount of produced starch, the effort to find new industrial applications is quite understandable (Šárka, Koláček, et al., 2012). In previous experiments B-starch was tested as a filler in biodegradable plastics (Šárka et al., 2011) and as a component of thermoplastic starch matrices (Kotek, Kruliš, & Šárka, 2011), i.e., in areas where starch has been applied recently (Chiellini, Chiellini, Cinelli, & Ilieva, 2003). The starch used in these studies was in native or in acetylated form because derivatisation decreases water absorption of films significantly (Tuovinen et al., 2004). Films prepared from acetylated starch require plasticisers different from those used frequently for native starch. A mixture of triethylcitrate and acetylated maltodextrin was proposed for this purpose (Kotek, Kruliš, Růžek, & Šárka, 2011). Besides modifying mechanical properties, acetylated maltodextrin also hinders degradation when compared with pure triethylcitrate (Šárka, Kruliš, et al., 2012).

Rutenberg and Solarek (1984) refers to amylolytic hydrolysis in combination with acetylation to produce acetylated maltodextrins or low molecular weight high-DS half-acetates made from hydrolysed starches with DE up to 40 for technical uses. A relationship of DS and DP is mentioned there.

The preparation and characterisation of natural and acetylated maltodextrin derived from wheat B-starch are aim of this paper. The average degree of polymerisation (*DP*), dextrose equivalent (*DE*) and degree of substitution (*DS*) are reported. *DE* measures the reducing power of sugars relative to a D-glucose (dextrose) standard on a dry mass basis. *DE* and *DP* values are related to molecular weight and are indicators of the degree of hydrolysis (Sun, Zhao, Zeng, Li, & Li, 2010).

* Corresponding author at: Department of Carbohydrates and Cereals, ICT Prague, Technická 5, 166 28 Prague 6 Dejvice, Czech Republic. Tel.: +420 220 443 115; fax: +420 220 445 130.
E-mail address: evzen.sarka@vscht.cz (E. Šárka).

0144-8617/$ – see front matter © 2013 Elsevier Ltd. All rights reserved.
http://dx.doi.org/10.1016/j.carbpol.2013.04.065

The properties and morphology of blends of a modified polymer with other polymers or additives depend strongly on the content of non-substituted groups, which have a compatibilising effect: consequently, physical properties of biodegradable composites containing acetylated carbohydrates will depend on *DS*. Therefore, FTIR (Chatel, Voirin, & Artaud, 1997) and ^{1}H NMR spectroscopy (Shogren, Stevenson, Willett, & Bhowmik, 2006) were used to study the extent of substitution of the acetylated maltodextrin.

Special attention was given to the assessment of product uniformity with respect to both molecular weight and composition because average *DP* and *DS* values do not convey complete information relevant to polymer or oligomer applications. Size exclusion chromatography (SEC) (Netopilik & Kratochvil, 2009), was used to determine the molecular weight distribution of the native and acetylated maltodextrins. For their low-molecular-weight components, MALDI-TOF mass spectrometry (Krupková, Čermák, Walterová, & Horský, 2007; Pasch & Schrepp, 2003) supplied information not only on the molecular weight distributions but also on the distribution of acetyl groups in the acetylated maltodextrin.

2. Experimental

2.1. Material

Dried wheat B-starch "Soltex P6" was provided by the Amylon Havlíčkův Brod starch company (Czech Republic; dry substance 91.3%, protein content 2.3%, acidity 73.9 mmol NaOH per kg of dry substance, mean average diameter of granules 5.9 μm).

Thermostable α-amylase "Liquozyme Supra" produced by *Bacillus licheniformis* (Novozymes A/S, Denmark; activity 135 KNU at 25 °C) was provided by the Amylon Havlíčkův Brod starch company (Czech Republic) as well.

Commercial acetic anhydride of purity 98.5% was purchased from Lach-Ner Limited, Neratovice (Czech Republic).

2.2. Hydrolysis of B-starch

B-starch was hydrolysed to the final DE of 18 using industrial thermostable α-amylase (EC 3.2.1.1). The enzyme was added to 1000 g of 20% (w/w) B-starch suspension at 90 °C and pH 7 to the final concentration of 0.68 g/kg DS starch. While keeping the suspension at 90 °C, 50 mL aliquots were collected at 10-min intervals and immediately inactivated by adjusting the pH to 4.0 with HCl. The final sample was obtained 120 min after the α-amylase addition and hydrolysis was promptly terminated. Each sample was frozen for storage and designated as B*X*, where *X* is the time of collection in min.

2.3. Acetylation of maltodextrin hydrolysates

The final hydrolysate was dried in a laboratory spray dryer (Armfield type FT30-A) at 150 °C, flow rate 7 mL/min through a nozzle of 0.5 mm. The dried product (dry substance of 92%) was acetylated using the procedure for starch acetylation described in Šárka et al. (2010). In contrast to the starch acetate, acetylated maltodextrin remained dissolved in exhausted acetanhydride. After pouring the reaction mixture into water, the yellowish precipitate was decanted, washed, dried at 40 °C, and designated as D13.

2.4. Methods

2.4.1. Determination of dextrose equivalent of hydrolysed starch

The dextrose equivalent (*DE*) of the hydrolysed starch samples was determined in accordance with Schoorl's method ISI 28-1e (http://www.starch.dk/isi/methods/28luff.htm, 8th November, 2012). The dependence of *DE* on the hydrolysis time was differentiated using the Origin 6.0 programme to obtain the hydrolysis rate.

2.4.2. SEC with aqueous mobile phase

Molecular weight distributions of the hydrolysed starch samples were determined by size exclusion chromatography (SEC) at room temperature. The SEC chromatography unit was equipped with a Deltachrom SDS 030 pump (Watrex, Czech Republic), guard column 50 mm × 7.5 mm PL aquagel-OH (Polymer Laboratories Ltd., USA), analytical columns 3× PL aquagel-OH 30, particle size 8 μm, 300 mm × 7.5 mm (Polymer Laboratories Ltd., USA). A Shodex RI 71 refractive index detector (Dionex Sofron GmBH, Germany) was used. The columns were eluted isocratically at a flow rate of 0.5 mL/min. A sodium phosphate buffer (0.01 mol/L, pH = 7) and sodium nitrate aqueous solution (0.2 mol/L) were used as the eluent. The injection volume was 100 μL. The chromatograms were evaluated by Clarity 2.4.1.87 (DataApex, Czech Republic). Monodispersed dextran standards were used to obtain a calibration curve.

2.4.3. SEC with tetrahydrofuran mobile phase

The SEC instrument used for determining the molecular weight of the acetylated maltodextrin (D13) consisted of a Deltachrom pump (Watrex, Czech Republic), a Midas autosampler with an injection-loop volume of 0.1 mL (Spark, Netherlands), a column system with ca. 4×10^2–10^7 applicability range – 50 mm × 8 mm GPC 10 μm guard column (Watrex, Czech Republic), two columns PL gel MIXED-B LS 10 μm particle size (Polymer Laboratories, USA) and a PL-ELS-1000 evaporative light scattering detector (Polymer Laboratories, USA). Tetrahydrofuran was used as the eluent at the flow rate of 0.5 mL/min. Measurements were carried out at ambient temperature. The data were accumulated and processed using TriSEC 3.0 software. Monodispersed polystyrene standards were used to obtain a calibration curve.

2.4.4. MALDI-TOF mass spectrometry

The dried droplet method (Pasch & Schrepp, 2003) was used: solutions of the sample (10 mg/mL), a matrix (2,5-dihydroxy benzoic acid, DHB; 20 mg/mL) and an ionisation agent were mixed in the volume ratio of 4:20:1, and 0.5–1 μL of the mixture was deposited on the ground-steel target plate and kept to dry. The solvent and ionisation agent were water and sodium chloride for the native maltodextrin and dimethylformamide and sodium trifluoroacetate for the acetylated maltodextrin, respectively. MALDI-TOF mass spectra were acquired with a Biflex III mass spectrometer (Bruker Daltonics) in the positive ion reflection mode, using delayed extraction. The spectra were the sum of 300 shots with an N_2 laser emitting at 337 nm and consisted of peaks corresponding to adduct with a single Na^+ ion.

2.4.5. ^{1}H NMR spectroscopy

The extent of the acetylation of maltodextrin D13 was determined by ^{1}H NMR spectroscopy in DMSO as described by Šárka et al. (2010) for acetylated starch, which is also suitable for highly acetylated samples. Briefly, a mass fraction of acetylated groups in the sample, OA_S, was determined from the integral of corresponding ^{1}H NMR signals using benzoic acid as an internal standard and then recalculated to *DS* following Wurzburg (1964)

$$DS = \frac{162 \times OA_S}{4300 - 42 \times OA_S} \quad (1)$$

where OA_S is expressed in %, 162 is the molecular weight of the anhydroglucose unit, and the other constants are derived from the molecular weight of the acetyl group.

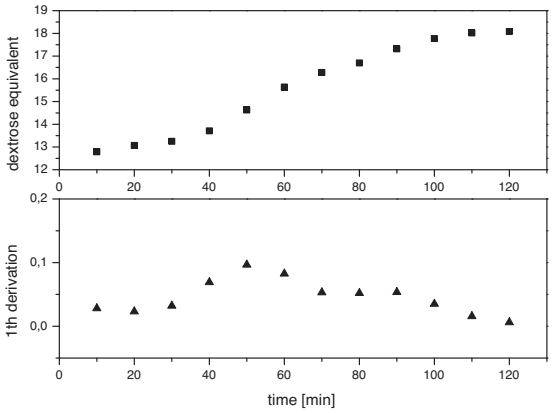

Fig. 1. Dependence of DE on time during wheat B-starch hydrolysis.

2.4.6. FTIR spectroscopy

FTIR spectra of the maltodextrin and its acetylated derivative were recorded in KBr tablets on a Nicolet 6700 FTIR spectrometer (ThermoScientific, USA) within the spectral range of 4000–400 cm^{-1} with a resolution of 2 cm^{-1} and the number of scans being 64. Obtained spectra were smoothed and the baseline corrected using Omnic 8.0 software (ThermoScientific, USA) and exported as CSW files to Origin 6.0 software (OriginLab, USA) for graph creation.

2.4.7. X-ray powder diffraction

X-ray powder diffraction data of the acetylated maltodextrin were collected at room temperature with an X'Pert PRO θ–θ powder diffractometer (PANalytical, Netherlands) with parafocusing Bragg–Brentano geometry using CuK_α radiation (λ = 1.5418 Å, U = 40 kV, I = 30 mA). Data were scanned with an X'Celerator ultrafast detector over the angular range 5–60° (2θ) with a step size of 0.017° (2θ) and a counting time of 20.32 s $step^{-1}$. Data evaluation was performed using the HighScore Plus software package.

3. Results

3.1. Hydrolysis kinetics

DE was determined in the samples taken every 10 min during enzyme hydrolysis of the B-starch. *DE* = 12.8 was found for the first sample, taken 10 min after the addition of α amylase, therefore the first and most intensive section of hydrolysis was not fully described, as can be seen in Fig. 1. This means that the hydrolysis rate was highest at the beginning of the hydrolysis because the *DE* of the original B-starch is practically zero. Subsequently, *DE* increased from 12.8 to 18.1 between 10 and 120 min (see Fig. 1). Surprisingly, the time dependence of *DE* in this time span was sigmoidal and the hydrolysis rate was at the maximum at about 50 min. Subsequently, the reaction rate fell and approached zero at 120 min.

3.2. Size exclusion chromatography

The SEC chromatograms of the B-starch hydrolysed for various times were all multimodal; those for 10, 70, and 90 min hydrolysis are shown in Fig. 2. Up to five peaks were identified in these chromatograms. Corresponding M_n (number-average molecular weight), M_w (weight-average molecular weight) and $PDI = M_w/M_n$ (polydispersity index) were calculated for samples B10–B120 using the Clarity 2.4.187 programme. Table 1 gives the results for the samples depicted in Fig. 2; for complete results see Supplementary data, Table 1. M_n ranged from 327,000 (Peak 1) to 237 (Peak 5); M_w from 370,000 (Peak 1) to 250 (Peak 2), and *PDI* from 1 (Peaks 4 and 5) to 2.4 (Peak 2). Peak 1, corresponding to the highest molecular weight, decreased with the time of hydrolysis and is almost absent from 60 min onwards. The change in hydrolysate composition during the hydrolysis, given as the relative area of peaks, is shown in Fig. 2d. Data presented here were obtained as an arithmetic mean of two values. The relative difference between the two measurements was less than 2%. The change occurred mostly between Peaks 2 and 3. The relative area of Peak 2 (M_w = 31,000) decreased from more than 40% to less than 30%; that of Peak 3 (M_w = 1200) increased in a similar way.

The chromatogram obtained for acetylated maltodextrin D13 is depicted in Fig. 3. The chromatogram is bimodal; the observable maxima are marked by arrows. The dash lines indicate the integration limits used to calculate molecular weight. The results of the chromatogram analysis are given in Table 2. The difference

Table 2
Results of characterisation acetylated maltodextrin D13 by size exclusion chromatography.

Peak[a]	M_p[b]	M_n[c]	M_w[d]	*PDI*[e]	*W*[f]
1	45,500	28,250	52,200	1.84	0.16
2	1750	1140	1820	1.60	0.84

[a] Peak number as given in Fig. 3.
[b] Molecular weight at peak maximum.
[c] Number average molecular weight.
[d] Weight average molecular weight.
[e] Polydispersity index.
[f] Mass fraction of the peak.

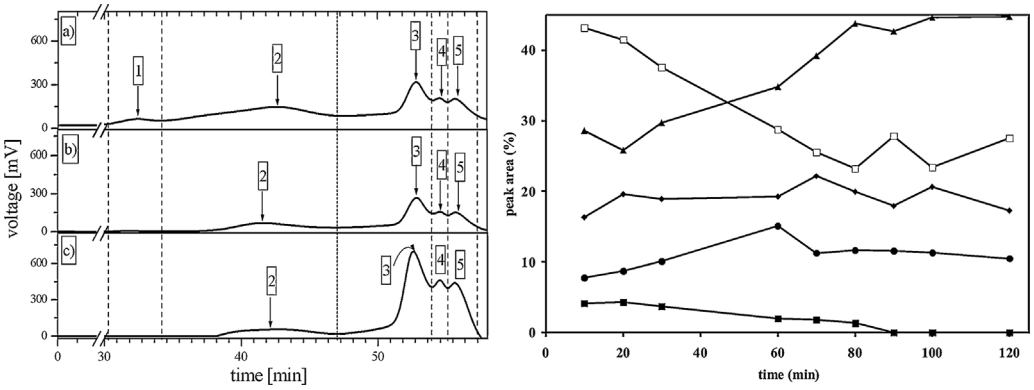

Fig. 2. SEC chromatograms of selected maltodextrin samples. The arrows indicate maxima of observable peaks; dash lines indicate the integration limits used in calculation of molecular weight averages. Samples: (a) B10 maltodextrin, (b) B70 maltodextrin, (c) B90 maltodextrin; (d) Change in relative peak areas during hydrolysis of B-starch. Symbols: ■ peak 1; □ peak 2; ▲ peak 3; ● peak 4; ♦ peak 5.

Table 1
Results of size exclusion chromatography of maltodextrins B10, B70, and B90.

Sample	B10				B70				B90			
Peak[a]	M_p[b]	M_n[c]	M_w[d]	*PDI*[e]	M_p[b]	M_n[c]	M_w[d]	*PDI*[e]	M_p[b]	M_n[c]	M_w[d]	*PDI*[e]
1	324,000	328,000	36,800	1.1	–	–	–	–	–	–	–	–
2	12,900	12,500	31,000	2.5	12,900	12,500	30,900	2.5	12,600	13,000	31,400	2.4
3	729	926	1167	1.3	745	911	1209	1.3	744	855	1141	1.3
4	394	408	415	1.0	410	420	425	1.0	410	410	414	1.0
5	285	238	246	1.0	293	237	251	1.0	294	237	254	1.0

[a] Peak number as given in Fig. 2.
[b] Molecular weight at peak maximum.
[c] Number average molecular weight.
[d] Weight average molecular weight.
[e] Polydispersity index.

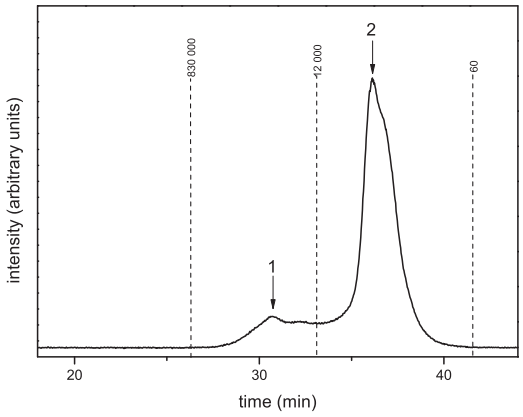

Fig. 3. SEC chromatogram of acetylated maltodextrin D13. The arrows indicate maxima of observable peaks. Dash lines indicate the integration limits used in calculation of molecular weight averages; molecular weights corresponding to the limits are also given.

in molecular weight between the two maxima is more than one order of magnitude (45,500 vs. 1750). The mass fractions of the higher-molecular-weight peak, estimated as the relative area under the curve, is 0.16.

3.3. MALDI-TOF mass spectrometry

The MALDI-TOF mass spectrum of maltodextrin B60 is presented in Fig. 4a. The spectrum consists of a series of peaks separated by 162 mass units and corresponding to various *DP* as expressed by Eq. (2) (Pasch & Schrepp, 2003)

$$M_{DP} = M_{EG1} + M_{MU}DP + M_{EG2} + M_{IA} \quad (2)$$

where M_{DP} is the molecular weight of maltodextrin with *DP* glucose units, M_{MU} is the molecular weight of a glucose unit, M_{EG1} and M_{EG2} are the molecular weights of end groups (together corresponding to H_2O for maltodextrins), and M_{IA} is the molecular weight of the ionisation agent (Na^+ in the present case). The spectrum reveals glucose polymer peaks with DP from 2 to 10, which is in accordance with data presented by Kennedy, Knill, and Taylor (1995). The peaks that are out of sequence at the beginning of the spectrum are considered to be due to the matrix adducts and disregarded. No signals were observed for the higher molecular weights, not even in the region of the molecular weight corresponding to Peak 2 as observed in the SEC chromatograms. Thus, information obtained by MALDI-TOF MS applies only to the low molecular-weight component of the sample. Nevertheless, the MALDI-TOF results represent approximately 75% of the entire sample on a mass scale, corresponding to more than 99% on a molar scale according to the SEC results.

Average molecular weights (number M_n or weight M_w), average degrees of polymerisation (number DP_n or weight DP_w), the polydispersity index (*PDI*), and the distribution of *DP* were determined from the MALDI-TOF mass spectra assuming that the relative peak area of a peak corresponding to a given *DP* equals the molar fraction of the polymer with this *DP* (Walterová & Horský, 2011). Values of M_n, M_w, DP_n, DP_w, and *PDI* obtained for maltodextrins

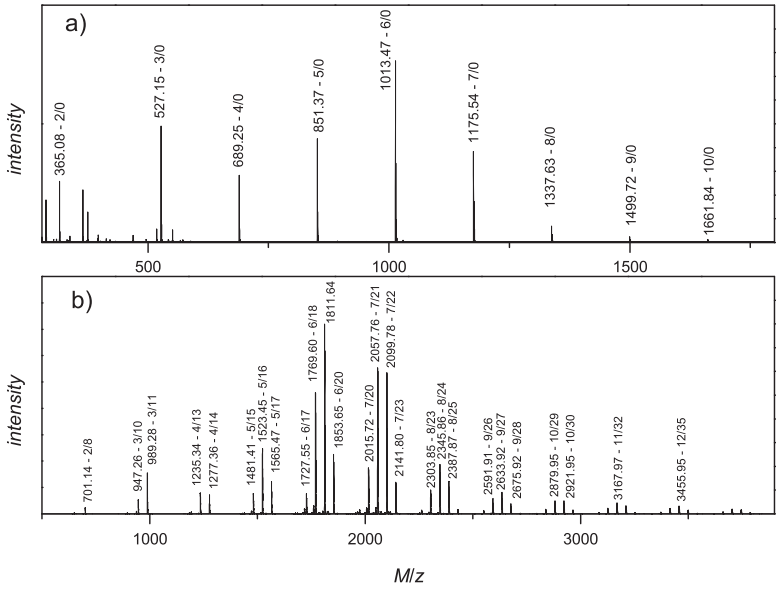

Fig. 4. MALDI-TOF mass spectrum (a) of native maltodextrin (B60), (b) of acetylated maltodextrin D13. Peaks labelling: $(M/z) - DP/(DP \times DS)$.

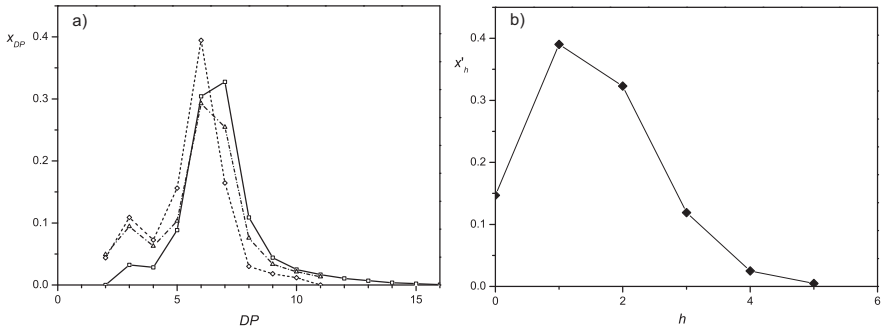

Fig. 5. (a) Number distribution of the degree of polymerisation for native maltodextrins B60 and B120 and for acetylated maltodextrin D13. Symbols: △ – B60; ◊ – B120; □ – D13. (b) Molar fraction x'_h of acetylated maltodextrin with a given number of unmodified hydroxyls h from MALDI-TOF MS.

B60 and B120 are given in Table 3, the distributions in Fig. 5. The potential effect of experimental conditions (Unterieser, Cuers, Voiges, Enebro, & Mischnic, 2011) on the results may be ignored because $PDI < 1.1$: it is generally accepted that molecular-weight distributions obtained by MALDI-TOF MS are reasonably accurate for samples with $PDI < 1.2–1.3$ (Pasch & Schrepp, 2003).

The MALDI-TOF mass spectrum of the acetylated maltodextrin (Fig. 4b) is more complex and consists of a series of peaks clustered in a way similar to the spectra of copolymers. As for the maltodextrins, the spectrum does not contain high molecular weight components. In this case, the MALDI-TOF mass spectrum represents 84% of the entire sample on a mass scale (more than 99% on a molar scale) according to the SEC results.

Average molecular weights can be calculated from the spectrum in the same way as with the unmodified maltodextrins (Table 3). In order to compare the original and acetylated maltodextrins, *DP* values are more useful. Despite the fact that partially acetylated maltodextrin may contain glucose units with varying numbers (up to 3) of acetylated hydroxyls, the spectrum was evaluated as that of a *binary* copolymer – namely, as a copolymer of unmodified glucose and modifying groups. *DP* and the number of modified groups, y, related to the degree of substitution *DS* by $y = DP \times DS$, were assigned to each isotopic cluster in the spectrum by Eq. (3)

$$M_{DP,y} = M_{EG1} + M_{MU}DP + \Delta My + M_{EG2} + M_{IA} \quad (3)$$

where ΔM is the increase in molecular weight due to the modification of one hydroxyl. It was thus possible to aggregate intensities of peaks corresponding to the same *DP* but different y and to calculate the average *DP* (Table 3) and *DP* distribution (Fig. 5a). Surprisingly, some small signals for $DP > 10$, entirely missing in the spectra of original maltodextrins, are detectable. Information on the extent of acetylation was obtained in a similar way – the average degree of substitution being DS_{AVG} (Table 3), or the number distribution of residual hydroxyls per molecule, h, which is more informative for highly acetylated samples than y, to which it is related by $h = 3DP + 2 - y$ (Fig. 5b).

Table 3
Characterisation of native and acetylated maltodextrins by MALDI-TOF mass spectrometry.

Sample	DP_n[a]	DP_w[b]	M_n[c]	M_w[d]	PDI[e]	DS_{AVG}[f]	h_{AVG}[g]
B60	5.95	6.52	983	1075	1.09	n.a.	n.a.
B120	5.52	5.96	913	984	1.08	n.a.	n.a.
D13	6.77	7.19	1990	2105	1.06	3.08	1.48

[a] Number average degree of polymerisation.
[b] Weight average degree of polymerisation.
[c] Number average molecular weight.
[d] Weight average molecular weight.
[e] Polydispersity index.
[f] Average degree of substitution (per glucose unit).
[g] Average number of residual hydroxyls (per molecule).

The value of DS_{AVG} calculated for the sample of acetylated maltodextrin D13 is higher than three because there are additionally two hydroxyls on the chain ends available for acetylation. The molar distribution of the maltodextrins with varying numbers of free hydroxyls is given in Fig. 5. It can be seen that most of the maltodextrin molecules have one or two free hydroxyls.

3.4. NMR spectroscopy

The proton NMR spectrum (Fig. 1 – Supplementary data) confirms the presence of acetyl substituents in the acetylated maltodextrin because methyl proton absorbance is present at 1.9 ppm. Comparing the integral area of these signals with that of benzoic acid added as an internal standard, DS_{AVG} was evaluated as 3.1.

3.5. FTIR spectroscopy

The IR band assignment in the spectra of maltodextrin and its acetylated derivative (Fig. 2 – Supplementary data) was made according to prior key sources (Capron, Robert, Colonna, Brogly, & Planchot, 2007; Chi et al., 2008). In the spectrum of maltodextrin, three bands at 1023, 1080 and 1155 cm^{-1} were attributed to CO stretching and COH bending vibrations. Further bands at 437, 526, 577, 608, 708, 763, 849 and 930 cm^{-1} arose from skeletal vibrations of the pyranoid ring. A broad band of OH stretching at 3386 cm^{-1} appeared due to hydrogen-bonded hydroxyl groups. It is evident that the acetylation led to significant changes in the spectrum of the derivative. IR bands of *O*-acetyls were found at 946 cm^{-1} (CH_3 rocking), 1242 cm^{-1} (COC stretching of ester), 1371 cm^{-1} (symmetric bending of CH_3), 1434 cm^{-1} (antisymmetric bending of CH_3), 1756 cm^{-1} (C=O stretching in the ester) and 2960 cm^{-1} (antisymmetric stretching of CH_3) (Chi et al., 2008). These bands were either absent or not pronounced in the spectrum of maltodextrin. The presence and high intensity of all these characteristic IR bands of *O*-acetyl substituents indicate a high degree of substitution for the derivatives of maltodextrin. The broad OH stretching band of maltodextrin of approximately 3386 cm^{-1} significantly decreased and shifted to 3470 cm^{-1} after acetylation. These changes indicate that most of the hydroxyls were substituted by acetyl groups. The water bending vibration band at 1647 cm^{-1} subsequently decreased with the acetylation and slightly shifted to 1645 cm^{-1}. The IR band at 1155 cm^{-1} was assigned to COC stretching vibrations in glycosidic bonds. This band was broadened and shifted to 1146 cm^{-1}. The region of 950–1130 cm^{-1} containing an envelope of highly overlapped bands (mainly CO and CC stretching vibrations in the pyranoid ring) was also sensitive to the substitution. The C1H bending band of maltodextrin at 849 cm^{-1} disappeared after substitution; a new skeletal vibration band was observed at 900 cm^{-1}.

3.6. X-ray powder diffraction

The measured X-ray powder pattern (XRD diffractogram) of the acetylated maltodextrin (Fig. 3 – Supplementary data) confirms the amorphous character of the precipitate, and this pattern is almost identical with acetylated wheat B-starch (Šárka et al., 2010).

4. Discussion

The hydrolysate was sampled at regular intervals primarily to verify that the required value of *DE* was achieved. Nevertheless, a kinetic curve was constructed from the data from 10 to 120 min after the addition of α-amylase and revealed rather peculiar behaviour. Initially unobserved rapid hydrolysis was followed by a period of relatively slow hydrolysis, after which its rate temporarily increased before falling to zero at its end. Evidently the kinetics of wheat B-starch hydrolysis by thermostable α-amylase is rather complex, when compared with A-starch reacting by different α-amylases coming from *B. licheniformis* or *Bacillus amyloliquefaciens* (Baks, Bruins, Matser, Janssen, & Boom, 2008; Besselink, Baks, Janssen, & Boom, 2008). The reasons trace back to the properties of both starch and α-amylase. The rate of hydrolysis depends on the mode in which the substrate binds to the α-amylase, which comprises several glucose-unit binding subsites around the catalytic site (Marchal, Ulijn, de Gooijer, Franke, & Tramper, 2003).

The comparison of A- and B-starch hydrolysis is not unambiguous in the literature. According to Manelius, Qin, Avall, Andtfolk, and Bertoft (1997) and Yonemoto, Calori-Domingues, and Franco (2007), despite their higher crystallinity small granules are more susceptible to hydrolysis than large ones, suggesting that the enzymatic susceptibility of small granules is related to its larger surface area. On the other hand Sakintuna, Budak, Dik, Yondem-Makascioglu, and Kincal (2003) found bigger starch granules (>30 μm) to be much more susceptible to hydrolysis than smaller ones (<10 μm). Our former kinetic measurements (Hrušková, 2011) confirmed the results of Manelius et al. (1997) and Yonemoto et al. (2007) for better starch hydrolysis of B-starch compared to A-starch up to 100 min, but after that time the hydrolysis of A-starch was faster.

Since one of the main objectives of the present study was to assess the uniformity of prepared acetylated maltodextrin and to discover how it was related to that of the original maltodextrin, the molecular weight distributions of hydrolysate samples were also investigated. Multimodal SEC chromatograms were obtained for all samples. In this respect, wheat B-starch behaves similarly to other starches (Cave, Seabrook, Gidley, & Gilbert, 2009). There may be several explanations for the multimodality. Multiplets at a low-molecular-weight region (Fig. 2, Peaks 3–5) most likely reflect the presence of individual maltodextrins in the hydrolysate, despite the fact that the molecular weights assigned to the peaks do not correspond to the theoretical molecular weight of the maltodextrins. Such agreement is, however, found by MALDI-TOF mass spectrometry, which shows that maltohexaose is the most abundant maltodextrin after 120 min. Nevertheless, the chromatograms are affected by lower SEC resolution: peaks are overlapping, and the assumption that each of them corresponds to a single maltodextrin is therefore unjustified.

The chromatographic Peaks 1 and 2, eluting at shorter times, in all probability reflect the bimodality of the molecular weight distribution of wheat B-starch. These two peaks are not observed in MALDI-TOF mass spectra because of the different type of detection. The differential refractometer used in SEC is sensitive to the mass concentration of analyte, whereas MS detectors are sensitive to the molar concentration. Hence, relative response to Peaks 1 and 2 will be lower by at least one or two orders of magnitude in MS than in SEC. Although the molecular weight of the two high molecular peaks must decrease during the initial stages of hydrolysis, it remained almost fixed in the studied span of *DE*; the progress of hydrolysis instead manifested mostly by the decrease of the peaks' relative areas – with Peak 1 completely disappearing. Nevertheless, Peak 2 still corresponded to approximately one quarter of the product mass even after 120 min of hydrolysis. SEC shows that the hydrolysis of high molecular components resulted in the increase of Peak 3. According to MALDI-TOF MS, the relative content of maltohexaose and maltopentaose increased between 60 and 120 min, while that of maltoheptaose decreased. The difference between SEC and MALDI-TOF MS seems to confirm that peaks in SEC do not correspond to single *DP*s.

Our finding that maltohexaose was a dominant component of hydrolysate after 120 min agrees with the results of Mironescu, Mironescu, Trifan, and Mironescu (2011), who determined by HPLC that the main products of liquefaction with "Liquozyme supra" are oligosaccharides with $DP \geq 5$. Nevertheless, the finding may not be taken as a final proof that "Liquozyme supra" is a maltohexaose-forming amylase even though the hydrolysis rate approached zero at 120 min according to *DE* measurements.

Both NMR and FTIR spectroscopy confirmed that highly acetylated ($DS = 3.1$) maltodextrin had been prepared. SEC showed that the molecular-weight distribution of D13 is bimodal. Peak 1 (Fig. 3) corresponds to Peak 2 of unmodified maltodextrin (Fig. 2) because the average *DP*s of those two peaks agree quite well despite the fact that polystyrene standards were used in the SEC of the acetylated maltodextrin. Peak 2 (Fig. 3) corresponds to Peak 3 (Fig. 2) according to the average *DP*s, but the asymmetry of Peak 2 (Fig. 3) suggests that it comprises the Peaks 4 and 5, too. The insufficient resolution of the acetylated maltodextrin of Peak 2 can be explained not only by the possibly lower resolution of the column system used for the SEC of the acetylated maltodextrin but also by the reflection of the acetylated maltodextrin's non-uniformity with respect to the *DS*, which is evident in its MALDI-TOF mass spectrum (Fig. 4).

The relative total area of signals corresponding to the acetylated maltodextrins with $DP > 6$ is larger in the D13 MS spectrum than in the MS spectrum of B120, in which signals for $DP > 11$ are missing. Calculated average *DP*s are, consequently, higher for D13 than for B120 by about 1.2. This indicates that partial fractionation occurred during acetylation, but the possible effect of composition on the MALDI-TOF MS response (Walterová & Horský, 2011) may be partly responsible for the shift.

The value of the average *DS* of D13 obtained by MALDI-TOF MS is in clear agreement with the NMR results despite the fact that 16% of the D13 mass is not accounted for by the MALDI-TOF MS. For some applications of acetylated maltodextrins, the exact content of residual hydroxyls, *h*, may be of great importance. MALDI-TOF MS determines h_{AVG} directly, not as $DS_{max} - DS_{AVG}$. The latter approach, which would need to be employed, e.g. with the NMR method used here, is limited by the dependence of DS_{max} on molecular weight and requires highly accurate values of DS_{AVG}. MALDI-TOF MS is therefore the method of choice for the determination of residual hydroxyls in the low-molecular-weight region, where uniformity with respect both to molecular weight and to *DS* or *h* can also be evaluated by MALDI-TOF mass spectra. It may be assumed that non-uniformity in the number of residual hydroxyls contributes to the amorphous nature of acetylated maltodextrin, as was similarly proposed for hydroxypropyl β-cyclodextrin (Irie et al., 1988).

5. Conclusions

The hydrolysis of wheat B-starch by α-amylase "Liquozyme supra" produced by *B. licheniformis* at 90 °C has complex kinetics with a rapid initial rate and is worth further investigation in

the context of a general study of starch hydrolysis by α-amylases. In addition to maltodextrins, the hydrolysate contains a significant amount of dextrins with $DP > 40$ even when DE approaches the upper limit for maltodextrins. This non-uniformity is then passed on to the product of the maltodextrin acetylation. Even if the acetylation has been carried out to a very high degree ($DS > 3$), most maltodextrin molecules still contain one or two unsubstituted hydroxyls. Hence, the non-uniformity of maltodextrins with respect to DP is combined with the non-uniformity in relation to DS in acetylated maltodextrins. The characterisation of acetylated maltodextrins and similar products therefore requires not only the use of complementary methods providing average values such as Schoorl's method and NMR, but also of separation methods which can provide information on uniformity, such as SEC, MALDI-TOF MS or HPLC. Each of these methods has some limitation and thus must be used in combination in order to provide a characterisation adequate for detailed understanding of the behaviour of modified polysaccharides and hence for the design of rational applications for them.

Acknowledgements

This research was supported by the "Biodegradable composites based on B-starch for agriculture applications "Research Grant, GAČR 525/09/0607.

Appendix A. Supplementary data

Supplementary data associated with this article can be found, in the online version, at http://dx.doi.org/10.1016/j.carbpol.2013.04.065.

References

Baks, T., Bruins, M. E., Matser, A. M., Janssen, A. E., & Boom, M. R. M. (2008). Effect of gelatinization and hydrolysis conditions on the selectivity of starch hydrolysis with alpha-amylase from *Bacillus licheniformis*. *Journal of Agricultural and Food Chemistry*, *56*, 488–495.

Besselink, T., Baks, T., Janssen, A. E. M., & Boom, R. M. (2008). A stochastic model for predicting dextrose equivalent and saccharide composition during hydrolysis of starch by alpha-amylase. *Biotechnology and Bioengineering*, *100*, 684–698.

Capron, I., Robert, P., Colonna, P., Brogly, M., & Planchot, V. (2007). Starch in rubbery and glassy states by FTIR spectroscopy. *Carbohydrate Polymers*, *68*(2), 249–259.

Cave, A. R., Seabrook, S. A., Gidley, M. J., & Gilbert, R. G. (2009). Characterization of starch by size-exclusion chromatography: The limitations imposed by shear scission. *Biomacromolecules*, *10*, 2245–2253.

Chatel, S., Voirin, A., & Artaud, J. (1997). Starch identification and determination in sweetened fruit preparations. 2. Optimization of dialysis and gelatinization steps, infrared identification of starch chemical modifications. *Journal of Agricultural and Food Chemistry*, *45*, 425–430.

Chi, H., Xu, K., Wu, X., Chen, Q., Xue, D., Song, C., Zhang, W., & Wang, P. (2008). Effect of acetylation on the properties of corn starch. *Food Chemistry*, *106*, 923–928.

Chiellini, E., Chiellini, F., Cinelli, P., & Ilieva, V. I. (2003). Biobased polymeric materials for agriculture applications. In E. Chiellini, & R. Solaro (Eds.), *Biodegradable polymers and plastics* (pp. 185–210). New York: Kluwer Academic/Plenum Publishers.

Galliard, T., Bowler, P., & Towersey, P. J. (1994). Minor components of wheat starch and their technological significance. In Y. Pomeranz (Ed.), *Wheat is unique* (pp. 251–262). St. Paul: American Association of Cereal Chemists.

Hrušková, K., Šárka, E., Pour, V., & Koláček, J. (2011). Laboratorní zkoušky přípravy maltodextrinu z pšeničného B-škrobu. In *Full texts of the 58th conference CHISA (CD ROM)* (p. 5). Srní, Czech Republic: Czech Society of Chemical Engineering.

Irie, T., Fukunaga, K., Yoshida, A., Uekama, K., Fales, H. M., & Pitha, J. (1988). Amorphous water-soluble cyclodextrin derivates: 2-Hydroxyethyl, 3-hydroxypropyl, 2-hydroxyisobutyl, and carboxamidomethyl derivatives of beta-cyclodextrin. *Pharmaceutical Research*, *5*, 713–717.

ISI 28-1e. (2012). *Determination of Reducing Sugar, DE by Luff-Schoorl's method*. Retrieved from: http://www.starch.dk/isi/methods/28luff.htm

Kennedy, J. F., Knill, C. J., & Taylor, D. W. (1995). Maltodextrins. In M. W. Kearsley, & S. Z. Dziedzic (Eds.), *Handbook of starch hydrolysis products and their derivatives* (pp. 65–82). London/Glasgow/Weinheim/New York/Tokyo/Melbourne/Madras: Chapma & Hall, Blackie Academic & Professional.

Knight, J. W., & Olson, R. M. (1984). Wheat starch: Production, modification, and uses. In R. L. Whistler, J. N. BeMiller, & E. F. Paschall (Eds.), *Starch: Chemistry and technology* (2nd ed., pp. 491–505). Orlando: Academic Press.

Kotek, J., Kruliš, Z., Růžek L., & Šárka, E. (2011). Biodegradovatelná kompozice na bázi modifikovaného škrobu a způsob její přípravy (Biodegradable composition derived from modified starch and process of its preparation). Patent Application CZ 2011-848, 20.12.2011.

Kotek, J., Kruliš, Z., & Šárka, E. (2011). Wheat B-starch based polymeric materials. In *Proceedings of the 7th international conference on polysaccharide-glycoscience* (pp. 37–39). Prague: Czech Chemical Society.

Krupková, A., Čermák, J., Walterová, Z., & Horský, J. (2007). Quantitative interpretation of MALDI-TOF mass spectra of imperfect carbosilane dendrimers. *Analytical Chemistry*, *79*, 1639–1645.

Leeb, C. V., & Schumann, H. P. (2007). Product design and engineering: Best practices. In U. Bröckel, W. Meier, & G. Wagner (Eds.), *Raw materials, additives and applications* (2) (pp. 395–419). Weinheim: Wiley-VCH.

Manelius, R., Qin, Z., Avall, A. K., Andtfolk, H., & Bertoft, E. (1997). The mode of action on granular wheat starch by bacterial alpha-amylase. *Starch/Stärke*, *49*, 142–147.

Marchal, L. M., Ulijn, R. V., de Gooijer, C. D., Franke, G. T., & Tramper, J. (2003). Monte Carlo simulation of the alpha-amylolysis of amylopectin potato starch. 2. Alpha-amylolysis of amylopektin. *Bioprocess and Biosystems Engineering*, *26*, 123–132.

Mironescu, M., Mironescu, I. D., Trifan, A., & Mironescu, V. (2011). Modelling of starch gelatinisation and liquefaction with the enzyme liquozyme. *Bulletin UASVMA Agriculture*, *68*, 327–332.

Netopilik, M., & Kratochvil, P. (2009). Models of SEC elution curves for binary and multi-component polymers. *Polymer International*, *58*, 198–201.

Pasch, H., & Schrepp, W. (2003). *MALDI-TOF mass spectrometry of synthetic polymers*. Heidelberg: Springer-Verlag.

Rutenberg, M. W., & Solarek, D. (1984). Starch derivatives: Production and uses. In R. L. Whistler, J. N. BeMiller, & E. F. Paschall (Eds.), *Starch: Chemistry and technology* (2nd ed., 2, pp. 311–388). Orlando: Academic Press.

Sakintuna, B., Budak, O., Dik, T., Yondem-Makascioglu, F., & Kincal, N. S. (2003). Hydrolysis of freshly prepared wheat starch fractions and commercial wheat starch using alpha-amylase. *Chemical Engineering Communications*, *190*, 883–897.

Šárka, E., & Bubník, Z. (2010). Morfologie, chemická struktura, vlastnosti a možnost využití pšeničného B-škrobu. *Chemicke Listy*, *104*, 318–325.

Šárka, E., Koláček, J., Sikora, A., Hrušková, K., Prokopová, D., Hrabal, R., Maixner, J., & Bubník, Z. (2010). Effect of reaction time on the acetylation of wheat B-starch and characterization of the product. In *Proceedings of the 6th international conference on polysaccharides-glycoscience* (pp. 200–205). Prague: Czech Chemical Society.

Šárka, E., Koláček, J., Hrušková, K., Kruliš, Z., Kotek, J., Růžek, L., & Růžková, M. (2012). Wheat B-starch: Application in biodegradable films. *Journal of Agricultural Science and Applications*, *1*, 45–48.

Šárka, E., Kruliš, Z., Kotek, J., Růžek, L., Růžková, M., Koláček, J., Hrušková, K., & Bubník, Z. (2012). Properties of a new biodegradable composite based on wheat B-starch. In *Proceedings of the 8th international conference on polysaccharides-glycoscience* (pp. 48–51). Prague: Czech Chemical Society.

Šárka, E., Kruliš, Z., Kotek, J., Růžek, L., Korbářová, A., Bubník, Z., & Růžková, M. (2011). Application of wheat B-starch in biodegradable plastic materials. *Czech Journal of Food Science*, *29*, 232–242.

Shogren, R. L., Stevenson, D. G., Willett, J. L., & Bhowmik, P. K. (2006). Ionic liquids as solvents for biopolymers: Acylation of starch and zein protein. *Carbohydrate Polymers*, *66*, 546–550.

Sun, J., Zhao, R., Zeng, J., Li, G., & Li, X. (2010). Characterization of dextrins with different dextrose equivalents. *Molecules*, *15*, 5162–5173.

Tuovinen, L., Ruhanen, E., Kinnarinen, T., Rönkkö, S., Pelkonen, J., Urtti, A., Peltonen, S., & Järvinen, K. (2004). Starch acetate microparticles for drug delivery into retinal pigment epithelium – In vitro study. *Journal of Controlled Release*, *98*, 407–413.

Unterieser, I., Cuers, J., Voiges, K., Enebro, J., & Mischnic, P. (2011). Quantitative aspects in electrospray ionization ion trap and matrix-assisted laser desorption/ionization time-of-flight mass spectrometry of malto-oligosaccharides. *Rapid Communication in Mass Spectroscopy*, *25*, 2201–2208.

Walterová, Z., & Horský, J. (2011). Quantification in MALDI-TOF mass spectrometry of modified polymers. *Analytica Chimica Acta*, *693*, 82–88.

Wurzburg, O. B. (1964). Acetylation. In R. L. Whistler (Ed.), *Starch* (vol. IV) *Methods in carbohydrate chemistry* (pp. 286–288). New York/London: Academic Press.

Yonemoto, P., Calori-Domingues, M. A., & Franco, C. M. L. (2007). Efeito do tamanho dos grânulos nas características estruturais e físico-químicas do amido de trigo. *Ciencia e Tecnologia de Alimentos*, *27*, 761–771.